28th AIAA Applied Aerodynamics Conference
28 June - 1 July 2010, Chicago, Illinois

AIAA 2010-4385

The Effect of Wing Spacing on Tandem Wing Aerodynamics

Timothy M Broering[1] and Yongsheng Lian[2]

University of Louisville, Louisville, KY 40292

This paper investigated the effect of wing spacing between fore and hind wings on a tandem wing configuration. The aerodynamics of flapping wings in tandem configuration was investigated numerically at Reynolds number of 5000. The flow field simulation was obtained by solving the incompressible Navier-Stokes equations on overlapping grids. Both convection and diffusion terms were discretized with second-order accurate central difference schemes. The tandem wing motion was handled with an overlapping moving grid. The tandem configuration was tested with four different wing gap spacings: 1.0, 0.5, 0.25 and 0.1 of the chord length. Aerodynamic force and power results as well as flow visualizations were shown. Adjusting the wing spacing had a noticeable effect on the resulting flow field and aerodynamic forces. As the wing spacing was decreased, vortex structures around the hind wing became elongated and spread out due to interactions with the fore wing. Total lift by tandem wings was maximized at a wing spacing of 1.0 while thrust was maximized at a spacing of 0.5. Power consumption was minimized at the closest wing spacing, 0.1. Surprisingly, the resultant force and propulsive efficiency of the tandem wings remained nearly constant across all wing spacings.

Nomenclature

c = wing chord length
U,u = fluid velocity
St = Strouhal number, $\frac{2fh_a}{U}$
f = flapping frequency
h_a = flapping amplitude
p = fluid pressure
ν = kinematic viscosity
F = body forces
Ω_0 = maximum angular velocity
t_0 = ramp interval to reach 99% of maximum angular velocity
t = time
h_0 = plunge amplitude
θ_0 = pitch amplitude
φ_h = phase lag between pitch and plunge
θ_{avg} = average pitch angle
C_L = lift coefficient
C_T = thrust coefficient

[1] Graduate Research Assistant, Department of Mechanical Engineering
[2] Assistant Professor, Department of Mechanical Engineering, Member AIAA

1. INTRODUCTION

Current research into micro air vehicles (MAV's) development has been fueled in large part by the success of unmanned air vehicles (UAV's) and the desire to replicate their functionality in a smaller form. Such small flight vehicles would have a number of potential uses such as reconnaissance and search and rescue missions, especially in urban environments, where their small size and maneuverability would allow them to operate within confined spaces. Their autonomous nature also lends them to operations in remote areas or hazardous environments. Development of such a vehicle that is maneuverable and capable of sustaining flight for a reasonable length of time presents a number of challenges. Due to the small dimensions and low flight speeds involved, MAV's operate at a much lower Reynolds number than conventional aircraft, which presents a challenge to traditional aerodynamic design.

MAV's operate at a low Reynolds number, on the same order as that of small birds and insects, where the increasing viscous effects lead to the development of complex flow phenomena. It has been shown that fixed wing vehicles become inefficient at low Reynolds numbers (under 100,000). [1] Since natural fliers utilize unsteady aerodynamics within this flow regime, the study of their various flight mechanisms provides a natural starting point for the study of MAV flight dynamics. At these low Reynolds numbers, moving airfoils generate and shed vortices from the leading and trailing edge, which can be exploited to enhance lift and thrust. [2] Indeed, various mechanisms of exploiting the generation and shedding of vortices, such as dynamic stall, clap and fling and wake capture, have been suggested as explanations for the high lift developed by certain natural fliers. [2,3]

Previous study in the area of flapping wing aerodynamics has predominantly focused on the aerodynamics of a single flapping wing. This is the type of arrangement favored by birds, which operate almost entirely in a turbulent flow regime. Insects, on the other hand, fly almost exclusively in a laminar flow regime, utilizing a variety of wing arrangements, including both single and tandem wing configurations. [4] This suggests that there is some advantage to using a tandem flapping wing arrangement to operate in a laminar flow regime. Perhaps the most iconic example of a natural tandem wing flier is the dragonfly, which exhibits the impressive performance that's possible utilizing a tandem wing configuration. Dragonflies are one of the most capable large flying insects. They have impressive maneuverability, are capable of hovering for extended periods of time and can even fly backwards.

The impressive flight performance of dragonflies has not escaped the attention of biologists or aerodynamicists. Both groups have investigated the wing anatomy, flight kinematics and performance capabilities of dragonflies. Norberg has provided morphological wing data, including wing shape, size, mass distribution, and weight. [5] Wakeling, Ellington, and Norberg have provided detailed kinematic data for dragonflies in both free forward flight and hovering. [5,6,7] Capturing high speed recordings of dragonflies in the field, May determined that they are capable of velocities of 10m/s, instantaneous accelerations of 4g and sustained accelerations of 2g. [8] Performing force measurements on tethered dragonflies, Reavis and Luttges measured dragonflies producing lift forces equal to 15-20 times their own body weight. [9] Thomas, et al. provided an in depth look at dragonfly flight dynamics by performing smoke visualizations on both tethered and free flying dragonflies. They determined that dragonflies generate high lift through the generation of leading edge vortices and that the behavior of these vortices is controlled via the angle of attack. [10] Specifically, they found that the formation,

growth and stabilization of the leading edge vortices were associated with increases in the angle of attack, while vortex shedding was associated with decreases in the angle of attack. This seemingly indicates that the generation and control of leading edge vortices is crucial to the flight abilities of dragonflies.

Dragonflies also have the ability to actuate each set of wings independently, enabling them to change the phase angle between the flapping cycles of each set of wings. It would seem that such a capability would be advantageous and, indeed, dragonflies have been observed making use of different phase shifts during flight. [11] Specifically, it has been noticed that dragonflies flap their wings inphase (0° phase difference between wing strokes) for high accelerations and flight maneuvers and flap their wings in counterstroke (180° phase difference between wing strokes) for cruising flight. This would suggest that inphase flapping increases the resultant force, while counterstroke flapping is more energy efficient.

The capability of dragonflies to adjust the phase lag between pairs of wings has not gone unnoticed in the field of flapping wing aerodynamics, and this capability is perhaps the most studied area in tandem flapping wing aerodynamics. Various studies have explored the effects of different phase lags for wings in both forward and hovering flight with some mixed results. Most cases have focused on how different phase shifts affect the lift and thrust and what phase lag produces the greatest amount of lift or thrust. By studying the vortex interactions between tandem wings, Saharon and Luttgess determined that the lift and thrust could indeed be controlled by altering the phase angle, thereby affecting the vortex interactions between wing pairs. [12-14]

It has been suggested that an inphase stroke produces higher aerodynamic forces and is used for energy demanding applications such as hovering, take off and load lifting. [15] Sun and Lan observed similar results through numerical simulation using a 2D Navier-Stokes solver with an overset grid method. [16] Furthermore, they found that a 90° phase lag produced the greatest horizontal force; however, the magnitude of the resultant force was decreased compared to a single wing. Also, while the inphase case produced the greatest resultant for the tandem cases the magnitude of the resultant force was almost unchanged compared to a single wing. Computational studies by Isogai and Shinmoto as well as Kim and Choi, showed that maximum lift is generated while hovering when the wings flap in phase. [17, 18] Solving the 3D Navier-Stokes equations for compressible flow using a moving overset grid method, Sun and Lan studied the aerodynamic force generation and power requirement of a dragonfly in hovering flight. They observed that the interaction between the fore and hind wings is not strong and is actually detrimental for hovering, decreasing the lift production by 14% and 16% on the fore and hind wings respectively. [19] Huang and Sun studied tandem wings in hovering mode using an overset grid method to solve the 3D Navier-Stokes equations and determined that the greatest lift was achieved at advanced phase angles where the fore wing had little effect on the hind wing. [20] At negative phase angles, the hind wing was greatly affected by the fore wing and the lift was greatly reduced. They observed that this was caused by the downwash of the fore wing reducing the effective angle of attack of the hind wing and may explain why dragonflies are observed using positive phase angles.

It has also been proposed that the observed phase shifts in the free flight of dragonflies is to make effective use of the hind wing to remove energy from the wake of the fore wing that would otherwise be lost. [21, 22] Using a double lattice method, Lan showed that two airfoils in

tandem produced increased lift and thrust at certain phase angle such that the hind wing can extract energy from the wake of the fore wing. [21] Work by Usherwood and Lehmann also noted that the hind wing can extract wake from the fore wing. Using an experimental model operating in hovering mode, Usherwood and Lehmann determined that the aerodynamic power requirements could be reduced by up to 22% for a tandem configuration versus a single wing for certain advanced phase angles. [22] They proposed that the increase in efficiency was achieved at certain phase angles where the hind wing recovered energy from the wake of the fore wing that was wasted as swirl.

While the effects of the phase lag on two airfoils operating in tandem has been studied extensively, the effects of the variations in the spacing between the two flapping airfoils has not. Adjustments to the wing spacing would likely have noticeable effect on aerodynamic performance. What the exactly are the effects of different spacing and what spacing is optimal for given flight kinematics are questions that have barely been investigated. For instance, an adjustment in the wing spacing could change the "effective" phase lag by altering at what point in the flapping cycle the wake of the fore wing reaches the hind wing. Also, as the spacing between the airfoils is decreased it is likely that the effects of the fore wing on the hind wing will become stronger. Determining an optimal spacing would be useful for the development of tandem wing configurations. Using an experimental tandem wing model, Warkentin and DeLaurier tested a tandem configuration using four different spacings. [23] For spacings of 0.39c and 1.126c, the tandem configuration showed similar performance; however, for the two spacings above one chord length, 1.9c and 2.65c, aerodynamic performance was degraded.

Given the general lack of data in tandem wing aerodynamics that covers the effect of wing gap spacing, the focus of this study covers the effect of different spacings on a tandem wing configuration. Specifically, a tandem wing arrangement using flat plates (0.05c thickness) is simulated at a chord based Reynolds number of 5000 with four different wing gap spacings: 1.0c, 0.50c, 0.25c, and 0.10c with both wings flapping inphase. The Strouhal number for the cases was 0.3. For each spacing, the aerodynamic force generation and power requirements are compared, as well as the differences in the resulting vortex interactions. Of particular interest are any correlations between the resulting vortex interactions and the force histories.

2. RESEARCH METHOD

2.1 Numerical Method

The flow problems were solved using the time dependent incompressible Navier-Stokes equations, a form of which is listed here.

$$u_t + (u \cdot \nabla)u + \frac{\nabla p}{\rho} = v\Delta u, \qquad \nabla \cdot u = 0 \tag{1}$$

where u is the flow velocity, p is the pressure, v is the kinematic viscosity and Δ represents the Poisson operator. The equations were discretized on an overlapping grid using a second order accurate central difference approximation to the velocity and pressure equations. Time stepping was accomplished using a second-order accurate split-step scheme with an Adam's predictor corrector time-stepping method. [24] For the Reynolds number studied, 10,000, the flow was assumed to be accurately modeled as a direct numerical simulation and no turbulence model was employed.

2.2 Overlapping Moving Grid

The wing flapping motion leads to a moving boundary problem. A moving grid approach is needed to dynamically update the computational grid to accommodate the wing motion and so an overlapping moving grid method is adopted. [25] This method uses boundary-conforming structured grids to achieve high-quality representations of boundaries. It employs Cartesian grids as the background grids so that the efficiencies inherent with such grids can be exploited. The irregular boundary associated with standard Cartesian grid methods takes the form of the interpolation boundary between overlapping grids. The use of overlapping grids is desirable for moving bodies because it is computationally less expensive than most other conventional approaches. Interpolation points are located in the overlap region between different grids and are used to couple the solutions. As the body moves, the grid associated with the body moves with it, meaning that only the interpolation points between overlapping grids must be recalculated as opposed to the need to regenerate the whole mesh, as may be necessary with other methods. The movement of the body is defined by a specified motion as indicated in subsequent sections.

Figure 1 shows a schematic of the grid used for the tandem wing analysis. An O-type grid was generated around the airfoil using a hyperbolic grid generation technique. A high resolution wake grid was used to capture wing-wing vortex interactions. Points were stretched to increase the grid density near the airfoil's surface to better resolve the boundary layer around the airfoil, while the wake grid and two background grids were of uniform density. The entire domain is 20 chord lengths in the x and y directions with the airfoil configuration centered in the domain. Boundary conditions were set to a uniform inlet condition with a constant velocity at the left side of the domain, and an outflow condition at the top, bottom and right side of the domain, where the velocity is extrapolated from inside the computational domain. A no-slip boundary condition was used for the surface of the airfoils.

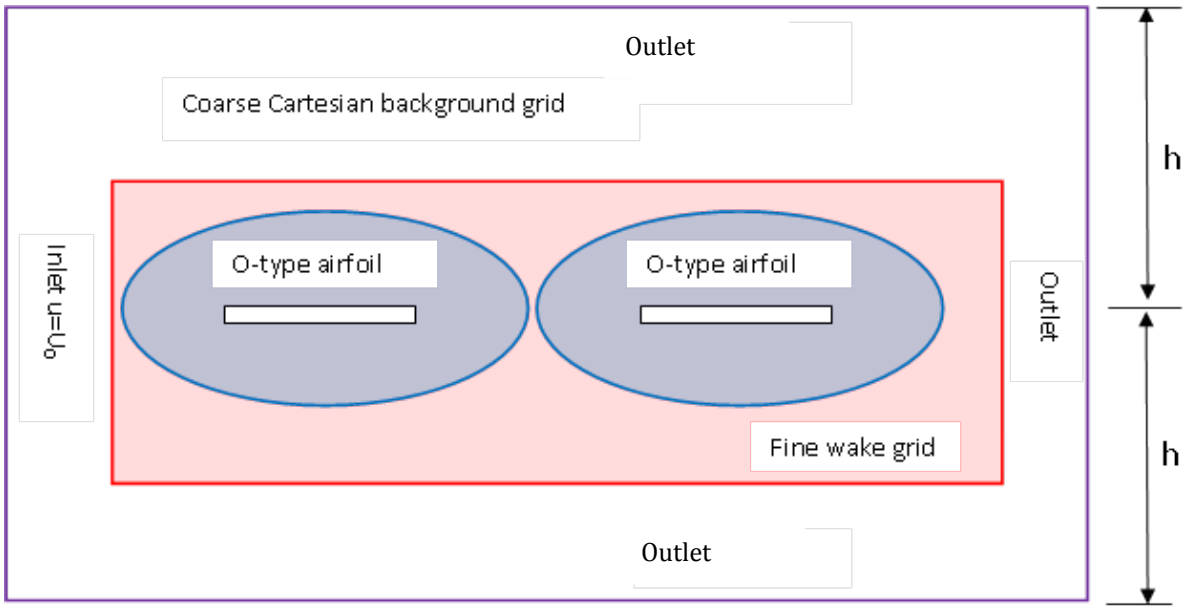

Figure 1. Schematic of the computational grid used for tandem wing analysis.

3.2 Airfoil Kinematic

The flapping kinematics used in the study was a combination of sinusoidal pitching and sinusoidal plunging. The equations of motion were

$$\alpha(t) = \alpha_0 \cos(2\pi f t + \phi_\alpha) + \alpha_{ave}$$

$$h(t) = h_0 \cos(2\pi f t + \phi_h)$$

where $\alpha(t)$ is the pitching angle, h(t) is the displacement, t is time, f is the flapping frequency, α_0 is the pitching amplitude, h_0 is the plunging amplitude, φ_α is the phase for pitch , α_{ave} is the average AoA, and φ_h is the phase for plunge. The parameters used for the kinematics are shown in Table 1.

Parameter	Value
α_0	20°
f	0.3
φ_α	90°
α_{avg}	5°
h_0	0.5
φ_h	0°

Table 1. Values used for the different parameters in the kinematic equations.

3.3 Grid Sensitivity Analysis

A grid sensitivity analysis was performed to determine which grid resolution was necessary to provide accurate force data as well as to resolve the flow field around the airfoils. The same kinematics were used for the sensitivity analysis as were used for the tandem wing cases, but only a single airfoil was used for the sensitivity analysis. As shown in Figure 2, four different grid configurations were tested. Note that the computational grids shown in Figure 2 are only to give an idea of the different types of grid structures used and are not the actual computational grids used in the analysis.

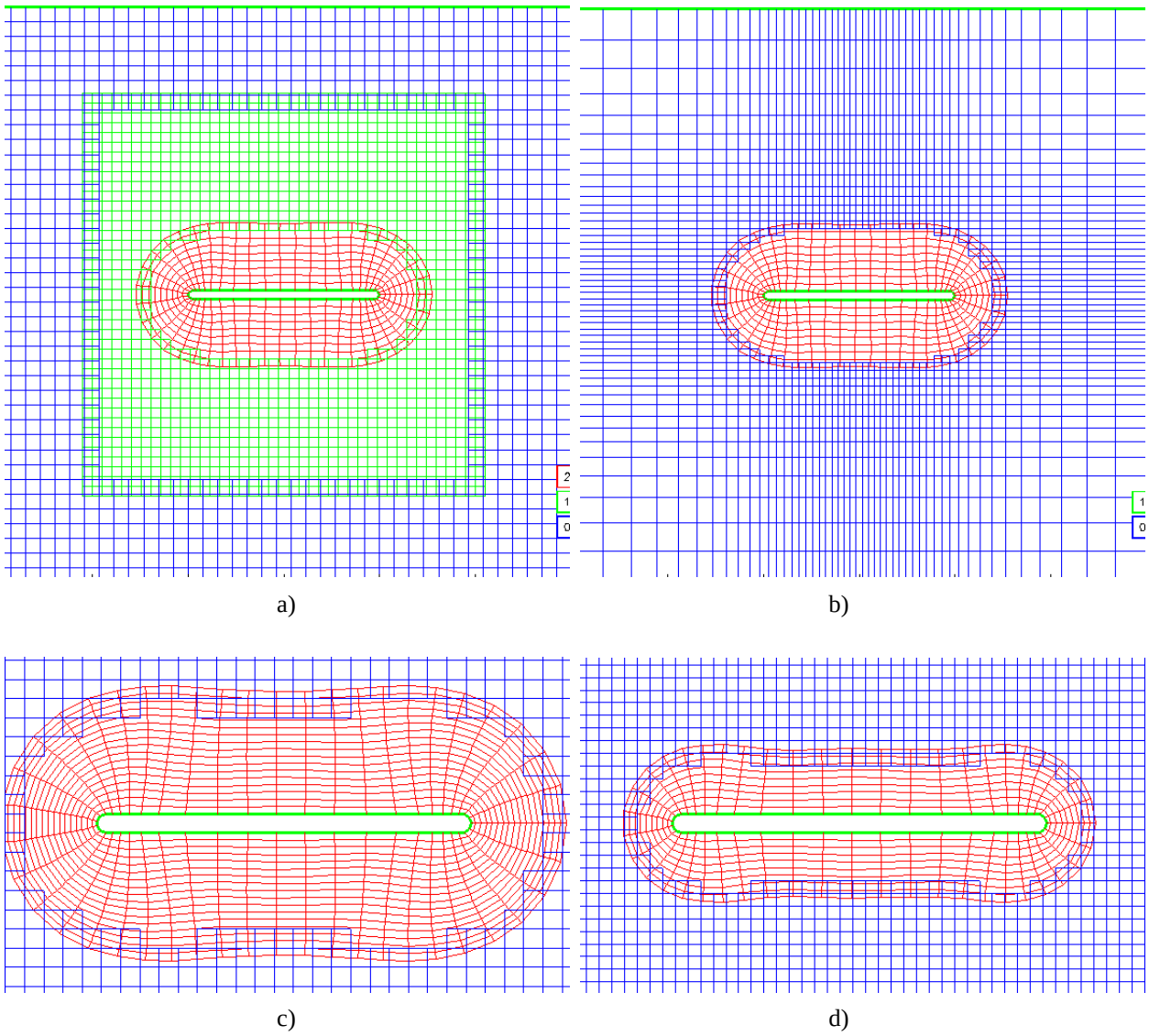

Figure 2. The different types of computational grids used in the sensitivity analysis. a) with uniform wake and background grids, b) with a stretched background grid, c) with a normal sized airfoil grid, d)with a small sized airfoil grid.

Different airfoil and wake grid resolutions were tested and the convergence was checked. Coarse, medium and fine resolutions were tested for both the airfoil and wake grids. The different grid resolutions are summarized in Table 2.

Airfoil Grid		Wake Grid	
Coarse	100x50	Coarse	150x100
Medium	150x75	Medium	200x150
Fine	200x100	Fine	250x200

Table 2. Grid resolutions tested for the airfoil and wake grid.

Figure 3 shows the lift and thrust coefficients for different airfoil and wake grid resolutions.

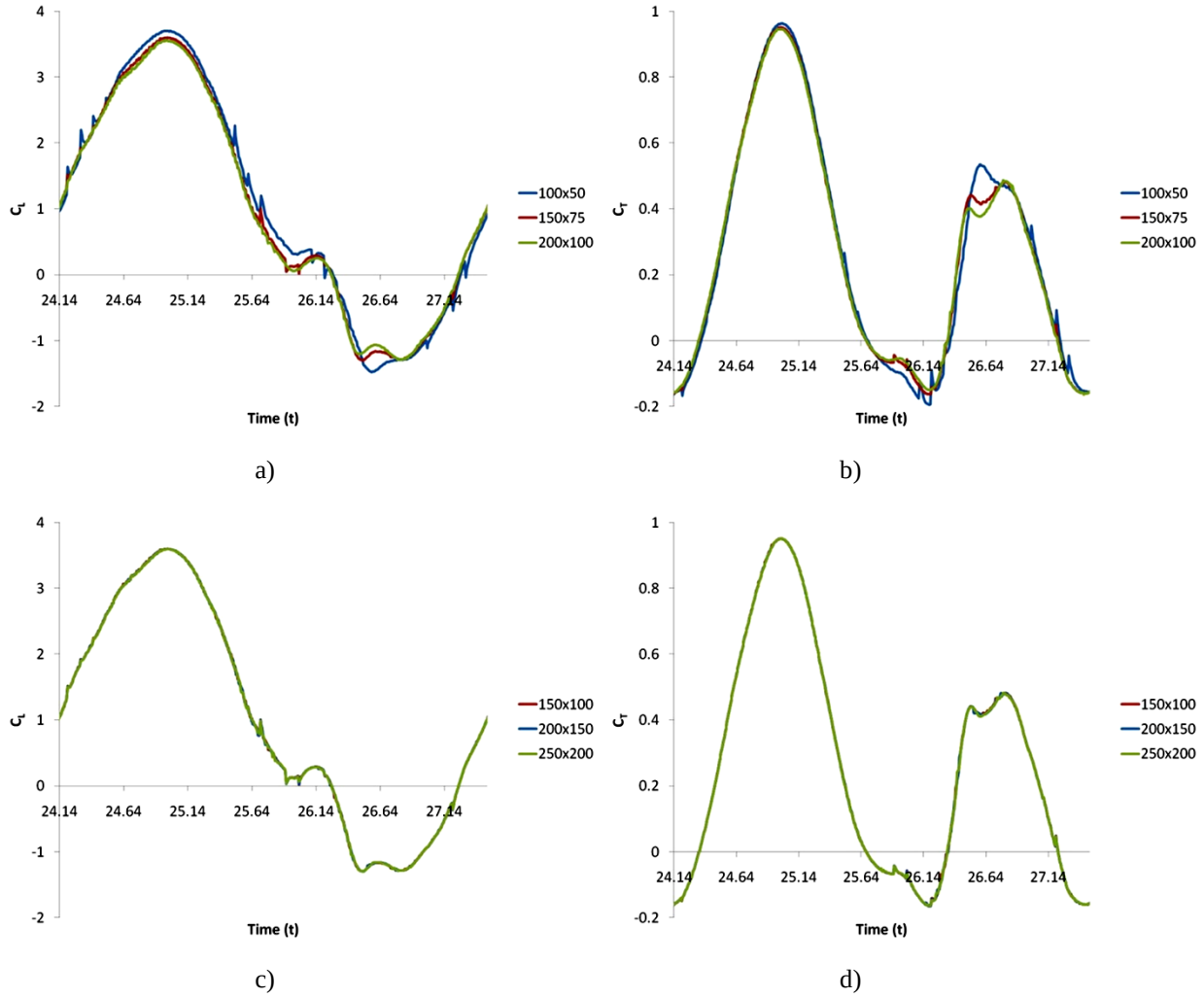

Figure 3. Lift and thrust data for grid sensitivity analysis. a)Lift for airfoil grids, b)thrust for airfoil grids, c)lift for wake grids, d)thrust for wake grids.

The tests showed that the forces were not sensitive to the wake grid resolution. Increasing the wake resolution from coarse to fine only change the forces by less than 1% (estimated from c and d). Changing the airfoil grid resolution did not greatly impact the force data at all, less than 2% difference between the medium and fine grid. The medium airfoil grid resolution was used for the rest of the study.

Figure 4 shows lift results for the different grid types overlaid with the results in Figure 3. The extra cases shown here are the small airfoil grid and the single stretched background grid cases. The data in Figure 4 shows that the different grid types did not have a noticeable impact on the force data. Neither getting rid of the wake grid nor decreasing the domain size of the airfoil grid structure visualizations.

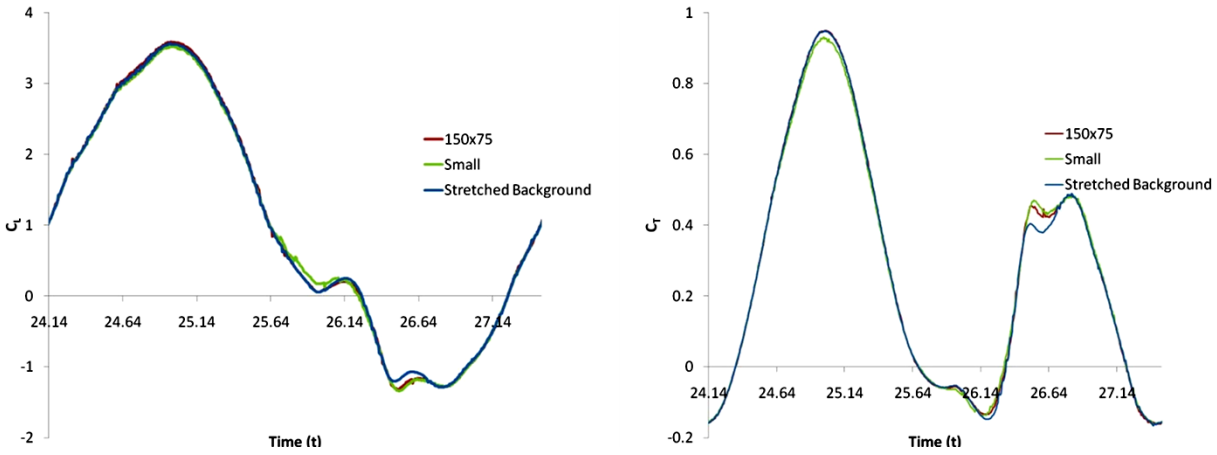

a) b)

Figure 4. Lift and thrust data for different grid types. a) lift, b)thrust.

Figure 5 shows the vorticity contours at the same point in the flapping cycle for the tested grid types.

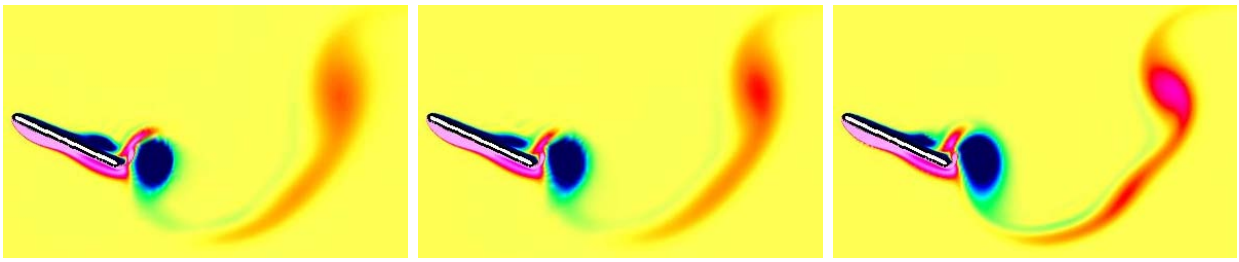

a) b) c)

Figure 5. Vorticity contours for the different grid types. a)with a stretched background grid, b)with a medium resolution wake grid, c)with a fine resolution wake grid and a smaller sized airfoil grid.

While the different grid types only had a negligible impact on the force data, Figure 5 shows that resulting vorticity contours depended greatly on the different grid type used. Using the single stretched background grid (Figure 5 a), the vortices dissipate quickly as they move downstream. Adding a wake grid behind the airfoil caused shed vortices to persist better into the wake with better definition (Figure 5 b), but the smaller sized airfoil grid with the fine resolution wake grid produced even better results displaying the most well defined vortex structures in the wake (Figure 5c). Since the hind wing performance can be significantly affected by the shed vortices from the fore wing, it is critical to capture the vortex structure. Based on the sensitivity analysis, it was decided to use the grid type utilizing the smaller sized airfoil grid and a fine resolution wake grid (Figures 2d, 5c) for the tandem wing analysis.

3. RESULTS

3.1 Effect of Wing Spacing on Time Dependent Forces

Figure 6 compares the force histories over a single flapping cycle for both the fore and hind wings for each of the different tandem wing spacings, 1.0, 0.5, 0.25, and 0.1. Each graph also shows the results for a single wing as a baseline reference,. Periodic motion had been established and the results shown here were taken during the eighth flapping cycle. The start of the cycle corresponds to the start of the downstroke and for all four spacings the wings were flapping inphase (0° phase).

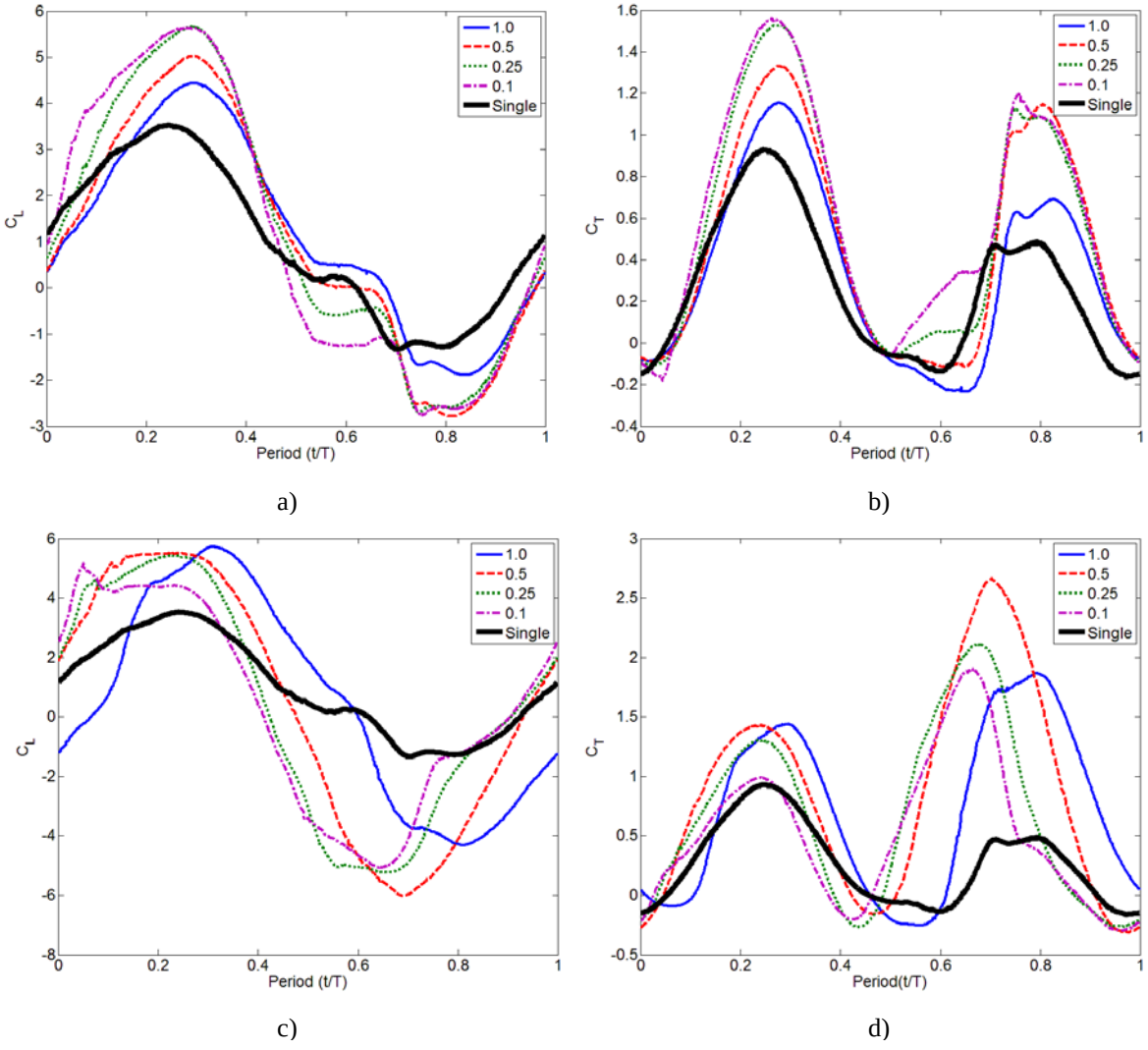

Figure 6. Time dependent force histories for the tandem configuration at different wing spacings compared to a single wing. a)fore wing lift, b)fore wing thrust, c)hind wing lift, d)hind wing thrust.

The following conclusions can be made about the effect of wing spacing on force histories

1. The fore wing has higher lift and thrust than the single wing at all spacings. This is consistent with previous observation. [26]
2. The hind wing effect on the fore wing increases with the decrease in wing spacing. But as the wing spacing is decreased to less than 0.25 chord, a further decrease in spacing does not produce any significant effect on the fore wing performance.
3. The fore wing effect on hind wing is mixed with the wing spacing.
4. Decreasing the spacing increases the peak lift and thrust magnitudes on both the fore and hind wings.
5. There was a slight phase shift in both lift and thrust curves for both fore and hind wings.

The effect of wing spacing on the lift and thrust production of the fore wing is clearly seen in Figure 6 a) and b). Compared to the single wing case, the fore wing of all tandem cases displayed higher lift and thrust.

3.2 Effect of Wing Spacing on Time Averaged Forces.

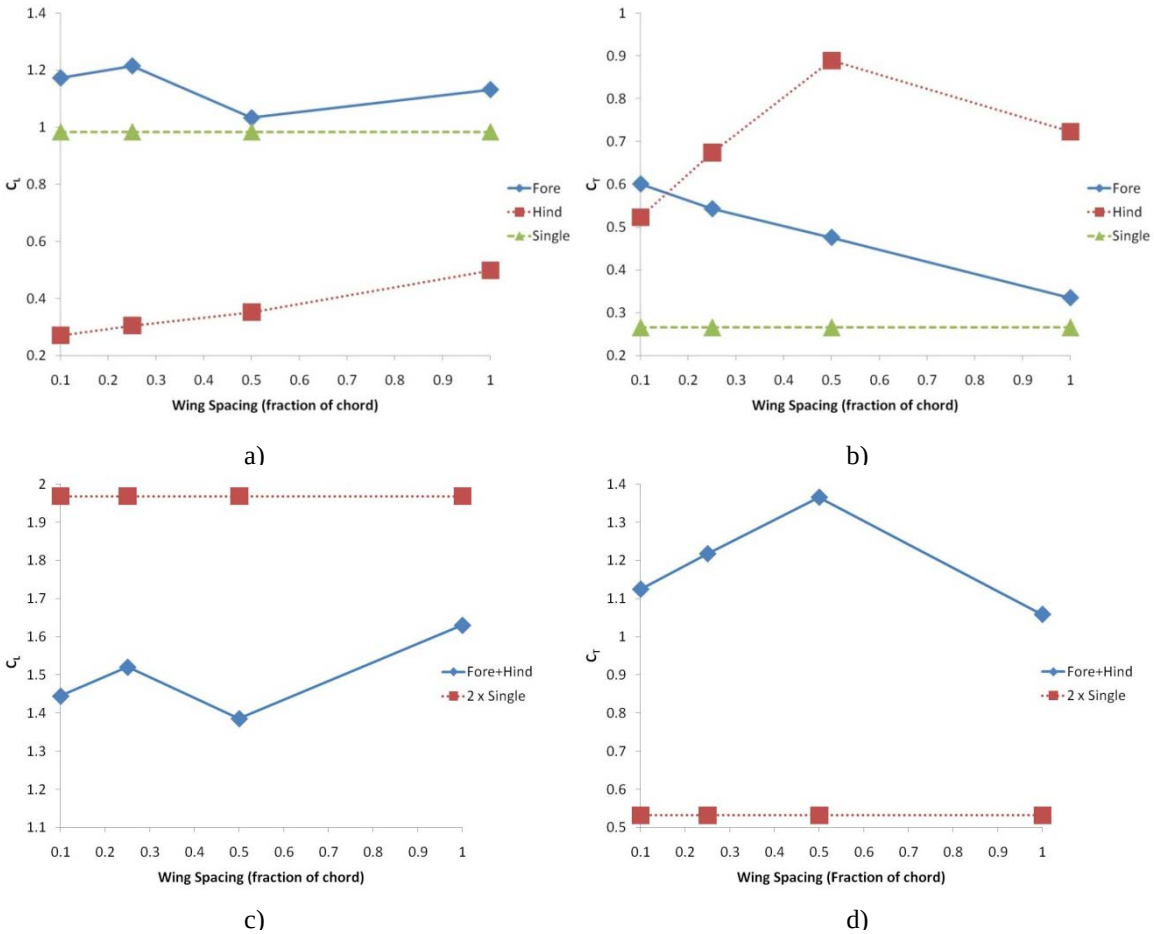

Figure 7. Time average lift and thrust at different wing spacings. a)average lift of fore/hind wing, b)average thrust of fore/hind, c)average lift of combined fore/hind wing, d)average thrust of combined fore/hind wing.

Figure 7 shows the time average lift and thrust values over a single flapping cycle versus the wing spacing. The graphs in a) and b) compare the lift and thrust values for the individual fore and hind wings to a single wing while the graphs in c) and d) show the lift and thrust values for the fore and hind wings combined compared to twice the same values for a single wing.

Analyzing Figure 7 results in the following conclusions

1. Lift production of the fore wing is just above that of a single wing for all spacings and tends to increase as the wing spacing decreases while the lift production of the hind wing is much lower than that of a single wing for all spacings and tends to decrease as the wing spacing decreases. Lift production was maximized at 0.25 for the fore wing and 1.0 for the hind wing.
2. The thrust production of both the fore and hind wings remain above that of a single wing for all wing spacings, but while the thrust production of the fore wing tended to increase with decreased wing spacing, the thrust production of the hind wing peaked at 0.5, then fell of quickly as the wing spacing was decreased to 0.25 and 0.1.
3. The results in c) and d) show that the tandem configuration produces significantly less lift for all wing spacings than the case of two isolated wings. To make up for this, it produces significantly more thrust, at least 100% more than the case of two isolated wings.
4. Comparing the different lift and thrust results at different spacings shows that the tandem wing configuration produced maximum lift at for a wing spacing of 1.0 and then tended to decrease with decreasing wing spacing. The thrust production of the tandem configuration; however, peaked at a wing spacing of 0.5 and then quickly deteriorated with further decreases in the wing spacing.
5. The resultant force produced by the tandem wing configuration was just less than that of two isolated wings for all the tested wing spacings (Figure 8). The resultant force of the tandem arrangement also remained remarkably constant for different wing spaces only decreasing slightly for the closest wing spacing, 0.1.

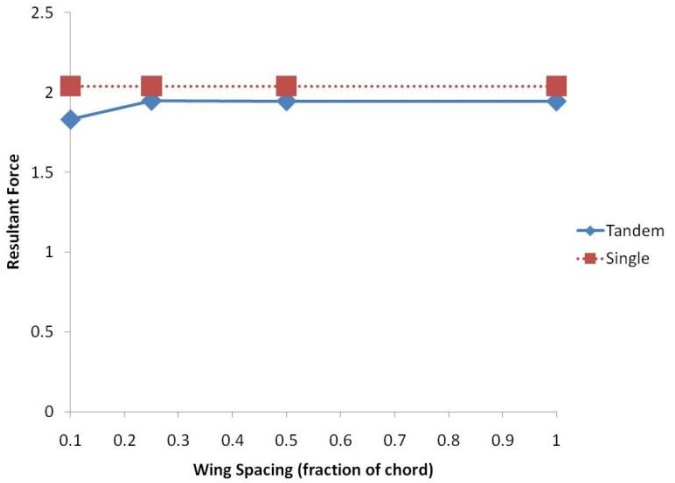

Figure 8. Resultant force of combined fore and hind wing at different wing spacings compared to twice the resultant of a single wing.

In summary, decreasing the wing spacing tended to increase the lift of the fore wing while decreasing the lift of the hind wing. The lift production of the fore and hind wings combined generally decreased with lower wing spacings and the lift for the tandem configuration was maximized at a wing spacing of 1.0. For thrust, the thrust of the hind wing peaked at a spacing of 0.5 and then rapidly fell off as the spacing was decreased further. On the other hand, the thrust of the fore wing increased as the wing spacing was decreased. The thrust production of the fore and hind wing combined was maximized at a wing spacing of 0.5. The effect of wing spacing on the resultant force was negligible.

3.3 Effect of Wing Spacing on Power Consumption

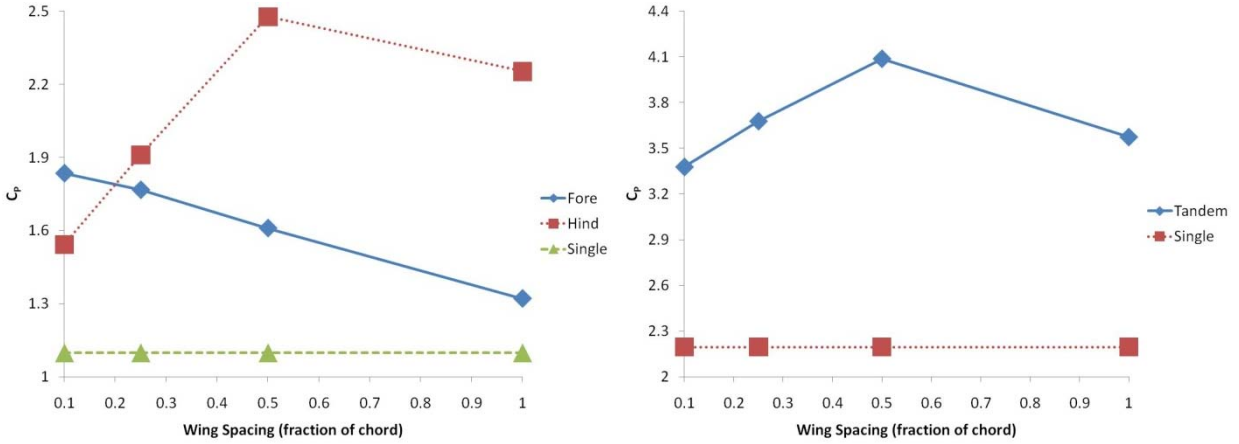

a) b)

Figure 9. Power consumption versus wing spacing. a)Power consumption of individual fore and hind wings compared to single wing, b)power consumption of combined fore and hind wing compared to two single wings.

Figure 9 shows the power coefficient, C_P, versus wing spacing for the individual fore and hind wing compared to a single in a) and for the combined fore and hind wing compared to twice the value for a single wing in b). C_P represents the input power into the wing (not the output power, which is thrust x velocity) and was calculated using

$$C_p = \frac{1}{0.5\rho A U^3}\int_0^T [-(L \cdot V) - (M \cdot \omega)]dt$$

where L is the lift force, V is the velocity due to plunge motion, M is the pitching moment and ω is the rotational velocity. The graph in Figure 9 a) shows that for the four different wing spacings, both the fore and hind wing had a greater C_P than a single wing. As the wing spacing was decreased, the power consumption of the fore wing was increased while the power consumption of the hind wing peaked at a wing spacing of 0.5 and then decreased sharply as the wing spacing was decreased further. For the combined tandem configuration, as shown in Figure 9 b), the power consumption at the four tested wing spacings was greater than that of two isolated wings. Also, the combined power consumption of the fore and hind wings peaked at a wing spacing of 0.5 before decreasing as the wing spacing was decreased further. It is interesting to note that the power consumption for the individual and combined wings follows

the exact same trend as the thrust production. That is Figure 2 b) and Figure 4 a) match up exactly as do 2d) and 4b).

Figure 10 shows the propulsive efficiency of the tandem configuration versus wing spacing compared to the same for a single wing. For the tandem configuration the propulsive efficiency remained nearly constant regardless of wing spacing. The propulsive efficiency of the tandem configuration also higher than a single wing for all tested wing spacings.

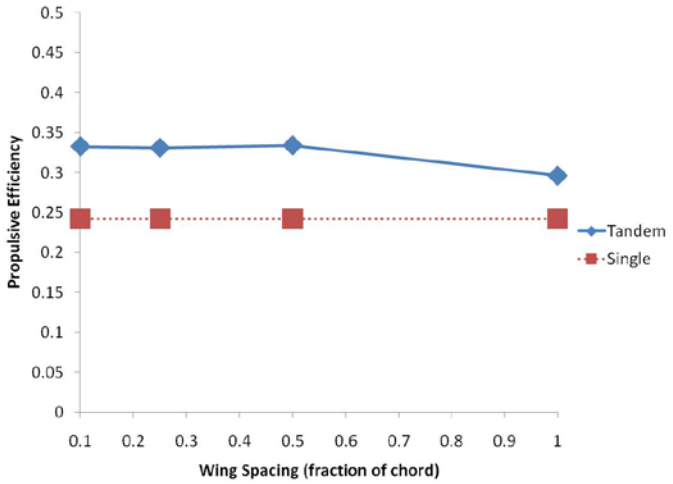

Figure 10. Propulsive efficiency of combined fore and hind wing at different wing spacing compared to a single wing.

3.4 Effect of Wing Spacing on Fore-Hind Wing Vortex Interactions

The figures below compare the vorticity contours between the different wing spacings for the tandem wing configuration. Four different snapshots from the flapping cycle are taken: the start of the downstroke (t/T = 0.0), the middle of the downstroke (t/T =0.25), the start of the upstroke (t/T = 0.5) and the middle of the upstroke (t/T = 0.75). Red colored contours represent counterclockwise (CCW) vorticity, while blue colored contours represent clockwise (CW) vorticity.

A number of conclusions are drawn from studying the figure.

1. At the start of the downstroke (t/T=0), decreasing the wing spacing increases the strength of the LEV on the fore wing but decreases the strength of the LEV on the hind wing. Furthermore, as the airfoils are moved closer together, the vortices around the hind wing are swept further below the wing, elongating the vortex structures.
2. At the middle of the downstroke (t/T=0.25) varying the spacing does not show change in the LEV on the fore wing. However, the strongest LEV occurs on the hind wing when the spacing is 0.25.
3. At at the start of the upstroke (t/T=0.5) varying the spacing does not show change in the LEV on the fore wing. But spacing effect on the hind wing is evident.
4. At the middle of the upstroke (t/T=0.75) as the spacing is decreased structured vortex pairs disappear from the wake of the hind wing.

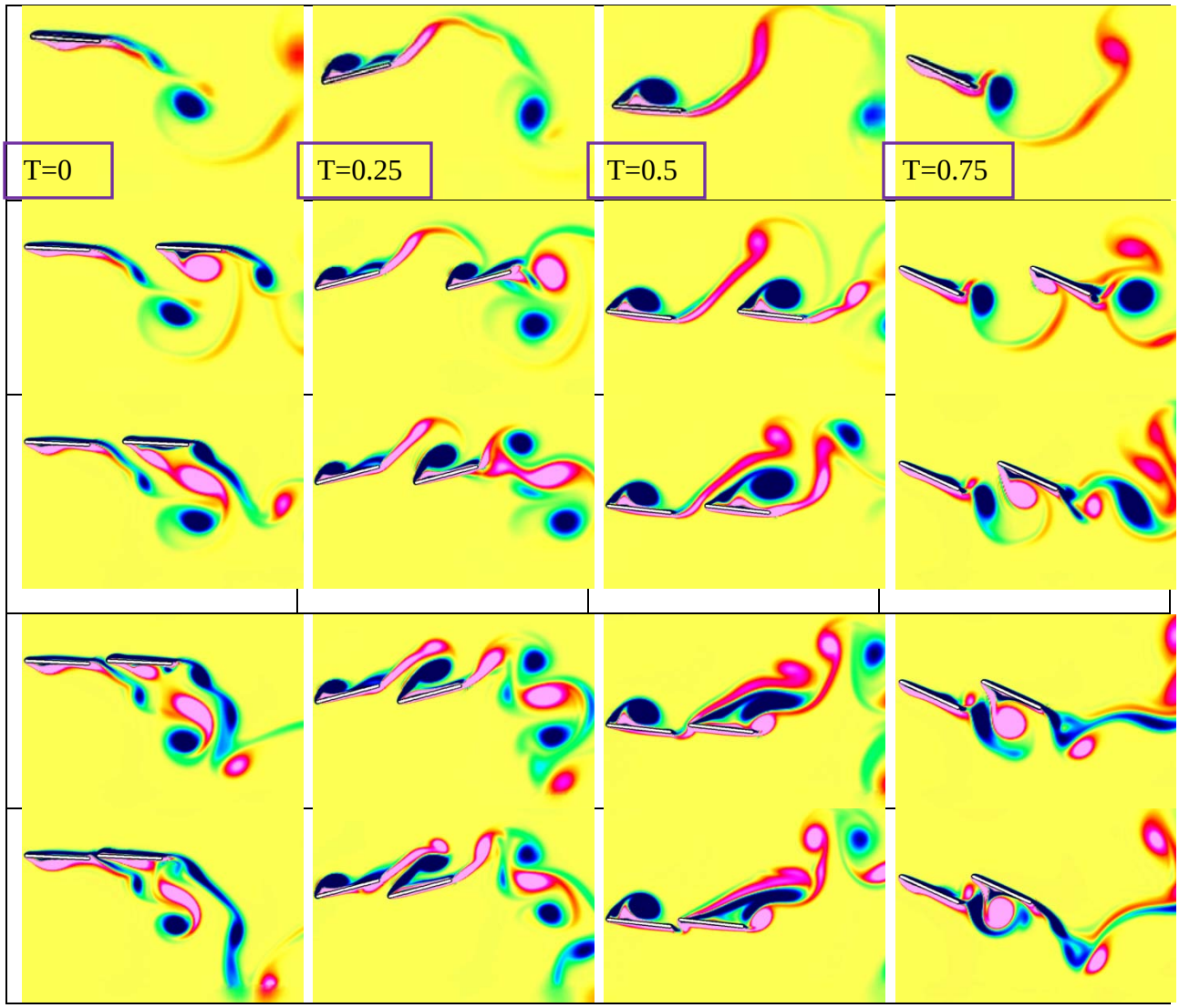

Figure 11. Vorticity contours of tandem wing configuration at the start of the downstroke. Row 1)Single wing, Row 2) 1.0 wing spacing, Row 3) 0.5 wing spacing, Row 4) 0.25 wing spacing, Row 5) 0.10 wing spacing.

Figure 11 shows the vorticity contours at four different time instants for the four different wing spacings. Here t=0 corresponds to the start of the downstoke, t=0.25 is the middle of the downstroke, t=-0.5 is the start of the upstroke,and t=0.75 is the middle of the upstroke.

At all the time instants, for a wing spacing of 1.0, vortex shedding from the fore wing interacts with like signed vorticity around the hind wing, increasing the size and strength of the CCW LEV formation on the underside of the hind wing. At t=0, the LEV formed on the bottom of the hind wing is pulled off the underside of the hind wing, and the vortices shed into the wake of the hind wing are drawn below the hind wing. At t=0.25, 0.5 and 0.75, there is also pairing of opposite signed vortices in the wake of the hind wing, indicative of thrust production.

Noticeable changes occur as the wing spacing is decreased. At t=0, the size of the CCW LEV formed on the bottom of the fore wing increases slightly; at t=0.25, the size of the LEV

formed on the top of the hind wing is increased (except for the closest wing spacing, where the LEV size decreases) and drawn further off of the fore wing; at t=0.5, As the wing spacing is decreased the LEV on the top of the hind wing is pulled off of the top of the hind wing and drawn into an elongated structure by the shedding of the vortex from the trailing edge of the fore wing; at t=0.75, when the wing spacing was decreased to 0.5, the LEV on the bottom of the hind wing decreased in size; however, the size of the LEV remained relatively constant as the spacing was decreased further. Decreasing the wing spacing to 0.5 also created a much larger pair of opposite signed vortices in the wake of the hind wing. As the wing spacing was decreased to 0.25 and 0.1, the same vortex structures became elongated and displaced outside of the wake directly behind the hind wing, creating a lack of well defined vortex structures in the wake of the hind wing.

At t=0.25, in the wake of the hind wing, opposite signed vortices still pair up at different wing spacings, but as the spacing is decreased the vortex pairing occurs further into the wake behind the hind wing. The size of the pair vortices also decreases as the wing spacing is decreased. At t=0.5, the pairing of vortex structures in the wake of the hind wing is also absent at the lower wing spacings as the vortices are drawn outside of the wake directly behind the hind wing. Closer wing spacings also cause the vortex shed from the trailing edge of the fore wing and the LEV of the hind wing to form up tightly together, creating a strong interaction of opposite signed vortices in the wake of the fore wing.

The resulting vortex interactions as the wing spacing was adjusted explain most of the changes in the force results. Considering the 1.0 spacing case first, this case displayed LEV generation at the hind wing that was larger and stronger than the typical LEV generation for a single wing (Figures 11 Row 1). These larger LEV's result in the larger lift force amplitudes on the down and upstroke for the 1.0 case compared to a single wing (Figure 6c). The 1.0 spacing case also resulted in a very structured vortex pattern in the wake of the hind wing with pairings of opposite signed vortices (Figures 1 Row 1). The hind wing passes in front of these pairing of vortices around the middle of both the up and downstroke causing the sharp rise in the thrust amplitudes (Figure 6d).

As the wing spacing was decreased, the closer proximity of the fore wing to the hind wing accelerated vortex growth around the hind wing, but also caused earlier leading vortex shedding from the hind wing, resulting in elongated vortex structures. This starts to become noticeable for the 0.5 spacing case (Figures 11 Row 2). Quicker LEV formation causes the slight phase shift in the lift force curve in Figure 6c and lift production increases earlier in the downstroke. As the LEV sheds away from the hind wing it becomes elongated and remains over the hind wing, prolonging the lift peak. This same behavior is seen on the upstroke, except the LEV is pulled further off the bottom of the hind wing (Figure 11 Row 2), causing a normal lift peak rather than the flattened lift peak observed during the downstroke. The 0.5 case also shows the same pairing of opposite signed vortex pairings in the wake of the hind wing though they are starting to become more unstructured. The thrust curve on the downstroke is unaffected compared to the 1.0 spacing, but there is a sharp rise in the thrust amplitude for the 0.5 case on the upstroke (Figure 6d). This is due to the vortex pairing in the wake of the hind wing shown in Figure 11 Row 2. Though the vortices are becoming unstructured, this vortex pairing is much larger for the 1.0 case, causing the larger thrust peak. This is also why the time averaged thrust peaks at a wing spacing of 0.5. The fore wing shows a similar increase in the thrust peak for the

0.5 case. This is due to the shed LEV from the fore wing interacting closely with an opposite signed LEV forming around the hind wing (Figure 11 Row 2).

Decreasing the wing spacing further to 0.25 causes increased vortex elongation which is seen in Figures 11 Row 3. The results are very similar to the 0.5 spacing case. Lack of structure vortex pairings in the wake of the hind wing (Figure 11 Row 3) decreases the thrust amplitude of the hind wing on the upstroke (Figure 6d). The thrust amplitude on the downstroke was also decreased slightly, due to the paired vortices being smaller and also situated further behind the hind wing (Figure 11 Row 3). While difficult to see, it is observable that the LEV formed on the top of the fore wing during the downstroke becomes tighter and better defined (Figure 11 Row 3), leading to an increase in the lift amplitude on the downstroke (Figure 6a). The fore wing also had a much larger thrust amplitude on the downstroke for a spacing of 0.25 than a spacing of 0.5. This was caused by the close interaction between the vortex shed from the trailing edge of the fore wing with the LEV starting to shed from the top of the hind wing which formed a pair of opposite signed vortices right in the wake of the fore wing (Figure 11 Row 3). This close interaction is a direct result of the decreased distance between the fore and hind wing.

When the wing spacing was decreased to 0.1, similar trends were seen compared to the other cases. The peak thrust amplitudes produced by the hind wing on both the upstroke and downstroke are the weakest of the four tandem wing cases (Figure 6d). On the downstroke, this is because the vortices in the wake of the hind wing are reduced in size and situated further into the wake behind the hind wing (Figure 11 Row 4). On the upstroke, the weak thrust amplitude of the hind wing is due to the complete lack of any structure vortex pairings in its wake (Figure 11 Row 4). The lift amplitudes from the hind wing on both the up and downstroke were also the weakest out of the four tandem wing cases (Figure 6c). This was caused by strong vortex interactions from the fore wing quickly displacing the LEV's from the hind wing, which weakened the lift production (Figures 11 Row 4). Vortex interactions and aerodynamic force production for the fore wing of the 0.1 wing spacing case were very similar to the same results for the 0.25 wing spacing case.

4. CONCLUSIONS

The wing spacing between fore and hind wing had a noticeable effect on the wing-wing vortex interactions and, consequently, the aerodynamic force production. As the wing spacing was decreased, the general effect on the fore wing was an increase in both the lift and thrust production. For the hind wing, on the other hand, the thrust peaked at a spacing of 0.5 while the lift decreased with decreasing wing spacing. Looking at the combined force production of the fore and hind wings, decreasing the wing spacing decreased the overall lift, while the thrust peaked at a spacing of 0.5. The resultant of the combined tandem configuration remained practically constant across wing spacing. Compared to twice the value of a single wing, the tandem configuration produced noticeably more thrust, significantly less lift and only a slightly smaller resultant across all wing spacings. Essentially the resultant of the tandem configuration was equal in magnitude to twice a single wing, but inclined more forward, at all four wing spacings. Finally, the propulsive efficiency of the tandem configuration was constant for all four wing spacings and was about 40% higher than the propulsive efficiency of a single wing.

5. ACKNOWLEDGEMENT

This work is partially supported by United State Air Force

REFERENCES

[1] McMasters, J. H., and Hendersen, M. L. *Low Speed Single Element Airfoil Synthesis*, Technical Soaring, Vol. 6, No. 2, pp. 1-21, 1980.

[2] Platzer, Max F., Jones, Kevin D., Young, John, Lai, Joseph C. S. *Flapping-Wing Aerodynamics: Progress and Challenges*, AIAA Journal, Vol. 46, No. 9, pp. 2136-2149, 2008.

[3] Viieru, Dragos, Tang, Jian, Lian, Yongsheng, Liu, Hao, Shyy, Wei. *Flapping and Flexible Wing Aerodynamics of Low Reynolds Number Flight Vehicles*, AIAA Paper 2006-503, Reno, NV, January 2006.

[4] Ellington, C.P., "Insects versus birds, the great divide," AIAA Paper 2006-35.

[5] Norberg, R. A., "Hovering flight of the dragonfly *Aeschna juncea* L," In *Kinematics and Aerodynamics*, vol. 2 (ed. T. Y.-T. Wu, C. J. Brokaw and C. Brennen), pp. 763-781. NY: Plenum Press, 1975.

[6] Wakeling, J. M. and Ellington, C. P. , "Dragonfly flight I: Gliding flight and steady-state aerodynamic forces," *Journal of Experimental Biology*, Vol. 200, pp. 543-556, 1997.

[7] Wakeling, J. M. and Ellington, C. P., "Dragonfly flight: II. Velocity, acceleration, and kinematics of flapping flight," *J. Exp. Biol.* Vol. 200, pp. 557–582, 1997.

[8] May, M. L. Dragonfly flight: power requirements at high speed and acceleration. *J. Exp. Biol. Vol.* 158, pp. 325-342, 1991.

[9] Reavis M.A., Luttges M.W., "Aerodynamic Forces Produced by a Dragonfly." AIAA Journal, Vol. 330, pp. 1–13, 1988.

[10] Thomas, Adrian L. R., Taylor, Graham K., Srygley, Robert B., Nudds, Robert L., Bomphrey, Richard J. *Dragonfly flight: free-flight and tethered flow visualizations reveal a diverse array of unsteady flight-generating mechanisms, controlled primarily via angle of attack*, The Journal of Experimental Biology, Vol. 207, pp. 4299-4323, 2004.

[11] Alexander, D.E. *Unusual phase relationships between forewings and hindwings in flying dragonflies*, Journal of Experimental Biology, Vol. 109, pp. 379-383, 1984.

[12] Saharon, D., and Luttges, M., *Three-Dimensional Flow Produced by a Pitching-Plunging Model Dragonfly Wing*, AIAA Paper 87-0121, Jan. 1987.

[13] Saharon, D., and Luttges, M., *Visualization of Unsteady Separated Flow Produced by Mechanically Driven Dragonfly Wing Kinematics Model*, AIAA Paper 88-0569, Jan. 1988.

[14] Saharon, D., and Luttges, M., *Dragonfly Unsteady Aerodynamic: The Role of the Wing Phase Relations in Controlling the Produced Flows*, AIAA Paper 89-0832, Jan. 1989.

[15] Ruppell, G., "Kinematic analysis of symmetrical flight maneuvers of Odonata," *J. exp. Biol*, Vol. 144, pp. 13-42.

[16] Lan, S. L. and Sun, M. "Aerodynamic force and flow structures of two airfoils in flapping motions," *Acta Mech. Sinica. Vol.* 17, pp. 310-331, 2001.

[17] Isogai, K., and Shinmoto, Y., *Study on Aerodynamic Mechanism of Hovering Insects*, AIAA Paper 2001-2470, June 2001.

[18] Kim, D., and Choi, H., *Vortical Motion Caused by Two Flapping Wings*, 2nd International Symposium Aqua-Bio-Mechanisms, Tokai University, Honolulu, Hawaii, Sept. 2004.

[19] Sun, M., and Lan, S-L. "A computational study of the aerodynamic forces and power requirements of dragonfly (*Aeschna juncea*) hovering," *Journal of Experimental Biology*, Vol. 207, pp. 1887-1901, 2004.

[20] Huang, Hua, and Sun, Mao. *Dragonfly Forewing-Hindwing Interaction at Various Flight Speeds and Wing Phasings*, AIAA Journal, Vol. 45, No. 2, 2007.

[21] Lan, C. E., *The Unsteady Quasi-Vortex-Lattice Method with Application to Animal Propulsion*, Journal of Fluid Mechanics, Vol. 93, No. 4, 1979.

[22] Usherwood, J., and Lehmann, F. O., *Phasing of Dragonfly Wings Can Improve Aerodynamic Efficiency by Removing Swirl*, Journal of the Royal Society, 2008.

[23] Warkentin, Jonathan, DeLaurier, James. *Experimental Aerodynamic Study of Tandem Flapping Membrane Wings*, Journal of Aircraft, Vol. 44, No. 5, 2007.

[24] Henshaw, W.D., and Petersson, N. A., "A Split-Step Scheme for the Incompressible {Navier-Stokes} Equations," *Numerical Simulation of Incompressible Flows*, World Scientific, pp. 108-125, 2003.

[25] Henshaw, W.D., and Schwendeman, D.W., "Moving Overlapping Grids with Adaptive Mesh Refinement for High-Speed Reactive and Non-reactive Flow," *Journal of Computational Physics*, Vol. 216**,** pp. 744-779, 2006.

[26] Broering T.M., Lian Y. "Numerical study of two flapping airfoils in tandem configuration." 48th AIAA aerospace sciences meeting including the new horizons forum and aerospace exposition. 2010, AIAA 2010-865.